Nagai Y, Asaoka Y, Namae M, Saito K, Momose H, Mitani H, Furutani-Seiki M, Katada T, Nishina H	The LIM protein Ajuba is required for ciliogenesis and left–right axis determination in medaka	Biochemical and Biophysical Research Communications	396	887–893	2010
Seo J, Asaoka Y, NagaiY,Hirayama J,Yamasaki T,NamaeM,Ohata S, Shimizu N, NegishiT,Kitagawa D,Kondoh H,FurutaniSeiki M,JM.Penninger KatadaTNishina H	Negative Regulation of wnt11 Expression by Jnk Signaling During Zebrafish Gastrulation	Journal of Cellular Biochemistry	110	1022–1037	2010
Negishi T, Nagai Y, Asaoka Y, Ohno M, Namae M, Mitani H, SasakiT,Shimizu N, Terai S SakaidaI Kondoh H, KatadaT Furutani-Seiki M,Nishina H	Retinoic Acid Signaling Positively Regulates Liver Specification by Inducing wnt2bb Gene Expression in Medaka	HEPATOLOGY	51	1037-1045	2010
Nakagawa K Sugahara M Yamasaki T Kajiho H Takahashi S Hirayama J Minami Y Ohta Y WatanabeT Hata Y Katada T Nishina H	Filamin Associates with Stress Signaling Kinases MKK7 and MKK4 and Regulates JNK Activation	Biochemical Journal	427	237-245	2010

Wu J Kubota J Hirayama J Nagai Y Nishina S Yokoi T Asaoka Y Seo J Shimizu N Kajiho H, WatanabeT Azuma N Katada T Nishina H	p38Mitogen-Activated Protein Kinase Controls a Switch betweenCardiomyocyte and Neuronal Commitment of Murine Embryonic Stem Cells by Activating Myocyte Enhancer Factor 2C-Dependent Bone MorphogeneticProtein 2 Transcription	Stem Cells and Development	19.11	1723-1734	2010
G. Gregory N, Kuba K, Cammarato A Isobe K, Sabine Zhang AL Murata M Elmén L Gupta V Arora S,Sarangi R Dan D Fujisawa S Usami T Xia C Keene AC Alayari NN Yamakawa H Elling U Berger C Novatchkova M Koglgruber R, Fukuda F Nishina H Isobe M Pospisilik JA Imai Y Pfeufer A Hicks AA Pramstaller PP Subramaniam S, Kimura A Ocorr K Bodmer R Penninger JM	A Global In VivoDrosophila RNAi Screen Identifies NOT3 as a Conserved Regulator of Heart Function	Cell	141	142-153	2010
Shimizu S, Konishi A, Nishida Y, Mizuta T, Nishina H, Yamamoto A, Tsujimoto Y	Involvement of JNK in the regulation of autophagic cell death	Oncogene	29	2070-2082	2010

MashimaR Honda K,YangY, Morita Y,Inoue A,Arimura S, Nishina H,Ema H, Nakauchi H, Seed B,OdaH, Yamanashi Y	Mice lacking Dok-1, Dok-2, and Dok-3 succumb to aggressive histiocytic sarcoma	Laboratory Investigation	90	1357-1364	2010
Tanemura S, Yamasaki T, Katada T Nishina H	Utility and limitations of SP600125,an inhibitor of stress-responsive c-Jun N-terminal kinase	Current Enzyme Inhibition	6	26-33	2010
YonedaS,Umemura T,KatsuyamaY,KamijoA,JoshitaS,KomatsuM,IchijoT,MatsumotoA,YoshizawaK,Ota M,Tanaka E.	Association of serum cytokine levels with treatment response to pegylated interferon and ribavirin therapy in genotype 1 chronic hepatitis C patients	J Infect Dis		In press	
Hattori E, Shu HJ, Saito T, Okumoto K, Haga H, Yokozawa J, Ito J, Watanabe H, Saito K, Togashi H, Kawata S	Expression of the RNA-binding protein Musashi1 in adult liver stem-like cells	Hepatol Res	40(4)	432-437	2010
Sanjo M, Saito T, Ishii R, Nishise Y, Haga H, Okumoto K, Ito J,Watanabe H,Saito K, TogashiH, Fukuda K,Imai Y,El-Shamy A, Deng L,Shoji I, HottaH Kawata	Secondary structure of the amino-terminal region of HCV NS3 and virological response to pegylated interferon plus ribavirin therapy for chronic hepatitis C	J Med Virol	82(8)	1364-1370	2010
Nishise Y, Saito T, Makino N, Okumoto K, Ito J, Watanabe H, Saito K, Togashi H,IkedaC,Kubota I, Daimon M, Kato T, Fukao A, Kawata S	Relationship between alcohol consumption and serum adiponectin levels: The Takahata Study - A cross-sectional study of a healthy Japanese population	J Clin Endocrinol Metab	95(8)	3828-3835	2010

Nishise S, Takeda Y, Fujishima S, Orii T, Sato T, Sasaki Y, Nishise Y, Takeda H, Kawata S	Release of interleukin 1 receptor antagonist by combining a leukocyte adsorption carrier with ulinastatin	Ther Apher Dial	14(4)	386-391	2010
Orii T, Takeda H, Kawata S, Maeda K, Yamakawa M	Differential immunophenotypic analysis of dendritic cell tumours	J Clin Pathol	63(6)	497-503	2010

The Lipid

別　刷

メディカルレビュー社
〒113-0034 東京都文京区湯島3-19-11
湯島ファーストビル TEL(03)3835-3041

Ⅱ. 基礎的メカニズムの解明
3. NASHと慢性炎症

東京医科歯科大学難治疾患研究所
分子代謝医学分野 特任助教
伊藤美智子

同 分子代謝医学分野 助教
菅波 孝祥

東京医科歯科大学難治疾患研究所
分子代謝医学分野 教授,
東京医科歯科大学グローバルCOEプログラム
小川 佳宏

[Summary]

肥満の進展過程において，肝臓では脂質蓄積・インスリン抵抗性に加え，組織常在性マクロファージであるクッパー細胞の活性化をはじめとした慢性炎症がNASH発症に関与していると考えられる．近年，肥満の脂肪組織や動脈硬化症など多くの肥満関連疾患の基盤病態として慢性炎症が注目され，病原体センサーTLR4と内因性リガンドの相互作用により誘導される「自然炎症」の病態生理的意義も明らかにされつつある．NASHは適切な動物モデルが存在しないため，NASHの進展とTLR4の関連は十分に検討されていない．今後，NASHにおける病態形成と「自然炎症」の関与が明らかになり，NASHの自然史が解明されることが期待される．

Key Words:
クッパー細胞□TLR4□自然炎症□飽和脂肪酸

はじめに

非アルコール性脂肪性肝炎（nonalcoholic steatohepatitis；NASH）は非アルコール性脂肪性肝疾患（nonalcoholic fatty liver disease；NAFLD）の中で，ときに肝硬変・肝癌に進展する重症型と考えられる．その発症機序としてTwo-hit theoryが提唱されているが，その詳細な発症メカニズムにはいまだ不明な部分が多い[1]．肝臓は糖脂質代謝において重要な臓器であるとともに，自然免疫系においても最前線として機能する臓器であり，NASHの病態には自然免疫が深くかかわっていると考えられる．近年，肥満，糖尿病や動脈硬化性疾患においてマクロファージの役割に対する理解が深まり，生活習慣病やメタボリックシンドロームに共通する基盤病態として「慢性炎症」が注目されている[2]．慢性炎症では，比較的短期間に炎症反応の活性化と退縮を生じる急性炎症と異なり，長期にわたるストレス応答のために実質細胞と間質細胞の相互作用が遷延化し，適応の破綻により不可逆的な「組織リモデリング」を生じて臓器の機能障害をもたらす．NASHは肝臓に脂質が蓄積し，肝細胞障害やクッパー細胞を含む免疫担当細胞の活性化により，肝星細胞が活性化して細胞外基質を過剰に産生し，線維化という組織リモデリングに至った状態と考えられる（図❶）．本稿では，組織常在性マクロファージであるクッパー細胞に焦点を当て，NASHの病態への関与と，

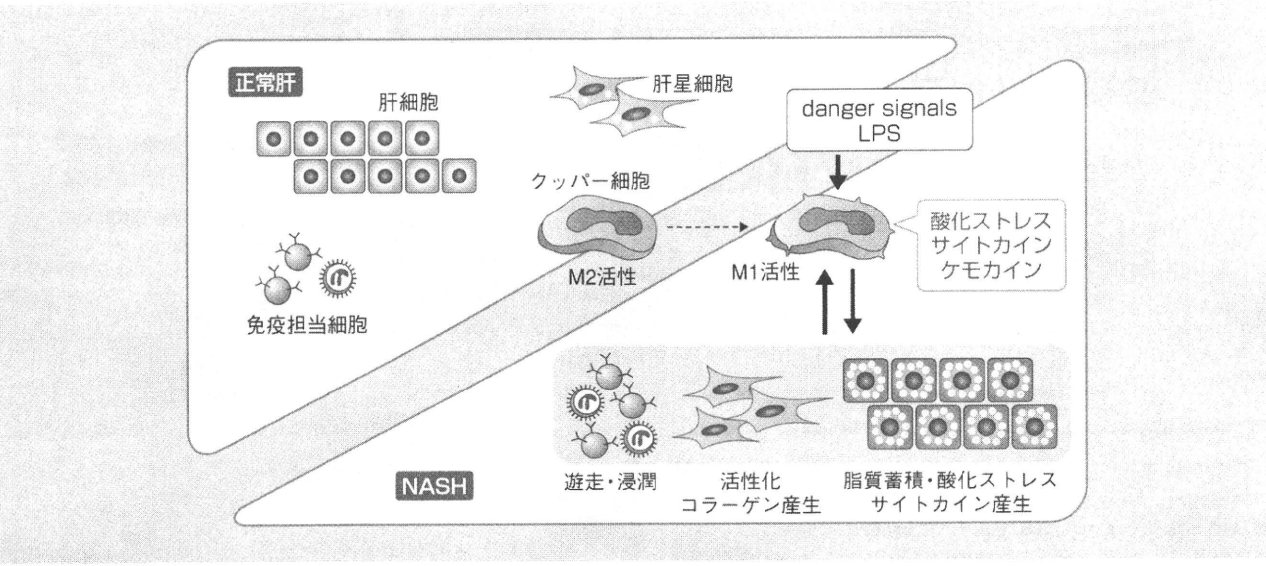

図❶　クッパー細胞の活性化と細胞間相互作用

正常肝は糖脂質代謝と自然免疫系を司る組織として，種々の細胞が恒常性維持に働いている．一方，肥満に伴って細胞障害によって放出されるdanger signalやLPSなどに曝されると，クッパー細胞は活性化し，さらに多くの酸化ストレス，サイトカイン，ケモカインなどを産生する．さまざまな細胞同士の相互作用の結果，炎症の遷延化・線維化といった組織リモデリングにつながる

病原体センサーと内因性リガンドの相互作用により誘導される「自然炎症」という新たな概念について述べる．

クッパー細胞と肝臓における炎症性変化

クッパー細胞は全身の組織常在性マクロファージの80~90%，肝非実質細胞の約10%を占める[3]．肝臓に流入する血流の約80%は門脈血であり，消化管由来の病原微生物，環境毒素，栄養素などが直接流入する．クッパー細胞は類洞に広く分布するため，生体に有害な物質を認識・除去することで，生体の恒常性維持に働いている[3]．具体的には，病原体やアポトーシス細胞，死細胞の残骸などの貪食や，活性酸素の産生による病原体の殺滅，ケモカイン産生による好中球や単球などの遊走を促す．また，抗原提示作用も有し，獲得免疫にも関与する．これらのクッパー細胞の機能は炎症応答を適正に調節するために厳格にコントロールされているが，慢性的な組織障害によってクッパー細胞の機能調節に破綻が起きると，さまざまな側面からNAFLDの病態形成に影響を与えることが予想される．

ガドリニウムやクロドロネートリポソーム法によってクッパー細胞を特異的に消去すると，四塩化炭素による肝障害や虚血再灌流障害，メチオニン・コリン欠乏食負荷における肝障害が軽減する[4,5]．これらの結果は，クッパー細胞がさまざまな肝障害モデルにおいて炎症と組織障害を増悪することを示している．一方で，四塩化炭素障害後の回復期にはクッパー細胞が組織修復を促進することから，障害の時期によって異なる役割を担っていると考えられる[5]．NASHのように慢性的なストレスによって発症する病態において，病態の進展過程で異なる役割をもつのかどうか，現在のところ明らかではない．また，上述の方法を用いて，高脂肪食あるいは高脂肪・高ショ糖食下にクッパー細胞を

消去すると，肝臓の中性脂肪含量が減少し，インスリン感受性が改善することが報告されている[6,7]．また，クッパー細胞と肝細胞の共培養系においてクッパー細胞を活性化させると，肝細胞における脂質合成系遺伝子の発現が増加し，β酸化が抑制されるということから，クッパー細胞が糖脂質代謝に影響を与え，脂肪肝そのものを促進していることが示唆される[7]．

マクロファージの活性化状態とNAFLD

マクロファージには炎症性サイトカインを産生する活性型のM1マクロファージと抗炎症性サイトカインを産生する非活性型のM2マクロファージがあり，病態に応じてマクロファージの性質に変化があると考えられている．例えば，非肥満の脂肪組織では非活性型のM2マクロファージが中心であるが，肥満に伴い増加する活性型のM1マクロファージは多くの炎症性サイトカインを分泌して脂肪組織の炎症性変化を促進するという[8,9]．このM1/M2極性に影響を与えるものとして，核内受容体であるperoxisome proliferators-activated receptor γ（PPARγ）やperoxisome proliferators-activated receptor δ（PPARδ）の関与が示唆されている[10,11]．PPARγあるいはPPARδを欠損するとマクロファージはM1側に傾き，高脂肪食負荷による肥満が誘導されやすく，インスリン抵抗性や脂肪肝が増悪する．特に，PPARδはクッパー細胞のM2極性に必要であるといわれている[11]．NAFLDの肝臓ではマクロファージにおけるM1サイトカイン産生増加が知られるが[7]，NASHにおいて常在性マクロファージの活性化と，浸潤マクロファージがそれぞれどのような影響を与えているのかは不明である．最近，脂肪肝では骨髄由来のC-C chemokine receptor 2（CCR2）陽性細胞が増加し，これらの細胞群はクッパー細胞に比較してM1サイトカインの産生が多く，肝中性脂肪含量の増加に関与していることが示された[12]．臨床的には，肥満や2型糖尿病の患者では循環血液中の単球の極性がM1様に変化していること，インスリン抵抗性改善薬であるチアゾリジン誘導体が単球の極性をM2様に変化させることが報告されており，循環血液中の単球の活性制御がメタボリックシンドロームの病態に関連する可能性が示唆されている[13,14]．

病原体センサーと自然炎症

Toll様受容体（toll-like receptors；TLRs）はパターン認識受容体ファミリーに属し，自然免疫系において病原体の認識と炎症性シグナル応答に重要であることが知られている[15]．特に，クッパー細胞に発現するTLR4は病原体センサーとしてグラム陰性菌の構成成分であるリポポリサッカライド（lipopolysaccharide；LPS）を認識し，細菌感染の免疫応答に中心的役割を果たす[15]．一方で，肥満の脂肪組織や動脈硬化症など非感染性の慢性炎症にTLR4が関与することが報告されている[16-18]．このような病態においては，自己の細胞から分泌される代謝産物，死細胞や細胞外基質より放出される因子（danger signal）が内因性リガンドとして作用していると考えられ，内因性リガンドに誘導される応答を「自然炎症」と捉える概念が提唱されている（図❷）．実際われわれは，脂肪細胞から放出される飽和脂肪酸がTLR4の内因性リガンドとして作用し，肥満脂肪組織におけるマクロファージとの相互作用や動脈硬化の初期病態とされる血管内皮への単球接着に関与することを報告した[19,20]．肝臓の線維化モデルとして汎用されるメチオニン・コリン欠乏食負荷モデルにおいても，TLR4を欠損すると肝脂質蓄積，炎症，線維化が改善する[21]．肥満では消化管において細菌の過増殖や消化管の透過性に変化が生じ，血中のLPS濃度が増加するといわれる[22]．消化管から流入したLPSは門脈を介して肝臓に到達するため，クッパー細胞はLPSの曝露を受け，これがNASH進展過程における2nd hitのひとつとして捉えられている[1]．一方で，NAFLD/NASHでは食物由来あるいは内臓脂肪での脂肪

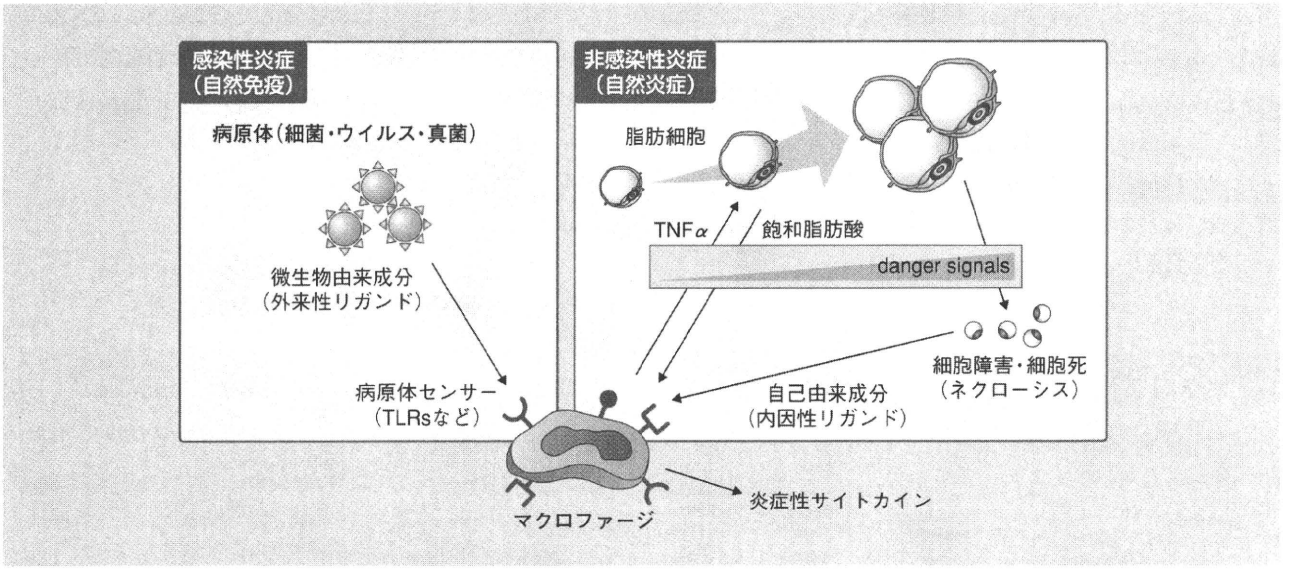

図❷ 肥満の脂肪組織における自然炎症

マクロファージの細胞表面上にはTLRsなどの病原体センサーを発現する．従来，病原体センサーは宿主には存在しない微生物由来成分をリガンドとすると考えられてきた(外来性リガンド)．しかしながら，細胞障害や細胞死(ネクローシス)など細胞が危機的な状況に陥ると，普段は放出されることのない自己由来成分(内因性リガンド)が「danger signal」として放出され，病原体センサーを介して慢性炎症を誘導・増悪する

分解に由来する脂肪酸の流入も増加していると考えられ，脂質を含むさまざまな因子が病原体センサーのリガンドとして作用している可能性がある．しかし，現在のところ，飽和脂肪酸以外にメタボリックシンドロームや動脈硬化の発症に関与するTLR4の内因性リガンドは不明であり，今後の重要な検討課題である．

おわりに

NASHの病態において，クッパー細胞をはじめとした自然免疫系の活性化と，肝細胞や肝星細胞など多彩な細胞との相互作用が深く関与している．そのメカニズムのひとつとして，クッパー細胞の病原体センサーTLRsとdanger signalの相互作用により誘導される「自然炎症」が経時的に増大していくと考えられる．また，TLRsはクッパー細胞だけでなく，肝星細胞にも発現しており，特に，胆管結紮モデルでは肝星細胞のTLR4が重要であることが報告されている[23]．NASHの臨床像を反映する適切な動物モデルが存在しないため，NASHの病態におけるTLRsの関与は十分検討されていない．今後，TLRsをはじめとした病原体センサーが，どのような細胞で何をリガンドとしてNASHの病態形成に関与しているかが明らかとなり，NASHの自然史が解明されることが期待される．

■文 献

1) Marra F, Gastaldelli A, Svegliati Baroni G et al: Molecular basis and mechanisms of progression of non-alcoholic steatohepatitis. *Trends Mol Med* **14**(2): 72-81, 2008
2) Hotamisligil GS: Inflammation and metabolic disorders. *Nature* **444**(7121): 860-867, 2006
3) Smedsrød B, De Bleser PJ, Braet F et al: Cell biology

of liver endothelial and Kupffer cells. *Gut* **35** (11): 1509-1516, 1994
4) Baffy G: Kupffer cells in non-alcoholic fatty liver disease: the emerging view. *J Hepatol* **51** (1): 212-223, 2009
5) Duffield JS, Forbes SJ, Constandinou CM et al: Selective depletion of macrophages reveals distinct, opposing roles during liver injury and repair. *J Clin Invest* **115** (1): 56-65, 2005
6) Neyrinck AM, Cani PD, Dewulf EM et al: Critical role of Kupffer cells in the management of diet-induced diabetes and obesity. *Biochem Biophys Res Commun* **385** (3): 351-356, 2009
7) Huang W, Metlakunta A, Dedousis N et al: Depletion of liver Kupffer cells prevents the development of diet-induced hepatic steatosis and insulin resistance. *Diabetes* **59** (2): 347-357, 2010
8) Lumeng CN, Bodzin JL, Saltiel AR: Obesity induces a phenotypic switch in adipose tissue macrophage polarization. *J Clin Invest* **117** (1): 175-184, 2007
9) Weisberg SP, McCann D, Desai M et al: Obesity is associated with macrophage accumulation in adipose tissue. *J Clin Invest* **112** (12): 1796-1808, 2003
10) Odegaard JI, Ricardo-Gonzalez RR, Goforth MH et al: Macrophage-specific PPARgamma controls alternative activation and improves insulin resistance. *Nature* **447** (7148): 1116-1120, 2007
11) Odegaard JI, Ricardo-Gonzalez RR, Red Eagle A et al: Alternative M2 activation of Kupffer cells by PPAR delta ameliorates obesity-induced insulin resistance. *Cell Metab* **7** (6): 496-507, 2008
12) Obstfeld AE, Sugaru E, Thearle M et al: C-C chemokine receptor 2 (CCR2) regulates the hepatic recruitment of myeloid cells that promote obesity-induced hepatic steatosis. *Diabetes* **59** (4): 916-925, 2010
13) Bouhlel MA, Derudas B, Rigamonti E et al: PPAR gamma activation primes human monocytes into alternative M2 macrophages with anti-inflammatory properties. *Cell Metab* **6** (2): 137-143, 2007
14) Satoh N, Shimatsu A, Himeno A et al: Unbalanced M1/M2 phenotype of peripheral blood monocytes in obese diabetic patients: effect of pioglitazone. *Diabetes Care* **33** (1): e7, 2010
15) Akira S, Takeda K: Toll-like receptor signalling. *Nat Rev Immunol* **4** (7): 499-511, 2004
16) Shi H, Kokoeva MV, Inouye K et al: TLR4 links innate immunity and fatty acid-induced insulin resistance. *J Clin Invest* **116** (11): 3015-3025, 2006
17) Suganami T, Mieda T, Itoh M et al: Attenuation of obesity-induced adipose tissue inflammation in C3H/HeJ mice carrying a Toll-like receptor 4 mutation. *Biochem Biophys Res Commun* **354** (1): 45-49, 2007
18) Björkbacka H, Kunjathoor VV, Moore KJ et al: Reduced atherosclerosis in MyD88-null mice links elevated serum cholesterol levels to activation of innate immunity signaling pathways. *Nat Med* **10** (4): 416-421, 2004
19) Suganami T, Tanimoto-Koyama K, Nishida J et al: Role of the Toll-like receptor 4/NF-kappaB pathway in saturated fatty acid-induced inflammatory changes in the interaction between adipocytes and macrophages. *Arterioscler Thromb Vasc Biol* **27** (1): 84-91, 2007
20) Yamada H, Yoshida M, Nakano Y et al: In vivo and in vitro inhibition of monocyte adhesion to endothelial cells and endothelial adhesion molecules by eicosapentaenoic acid. *Arterioscler Thromb Vasc Biol* **28** (12): 2173-2179, 2008
21) Rivera CA, Adegboyega P, van Rooijen N et al: Toll-like receptor-4 signaling and Kupffer cells play pivotal roles in the pathogenesis of non-alcoholic steatohepatitis. *J Hepatol* **47** (4): 571-579, 2007
22) Backhed F, Manchester JK, Semenkovich CF et al: Mechanisms underlying the resistance to diet-induced obesity in germ-free mice. *Proc Natl Acad Sci USA* **104** (3): 979-984, 2007
23) Seki E, De Minicis S, Osterreicher CH et al: TLR4 enhances TGF-beta signaling and hepatic fibrosis. *Nat Med* **13** (11): 1324-1332, 2007

LODISH・BERK・KAISER・KRIEGER
SCOTT・BRETSCHER・PLOEGH・MATSUDAIRA

分子細胞生物学

第6版

石浦章一・榎森康文・堅田利明
須藤和夫・仁科博史・山本啓一 訳

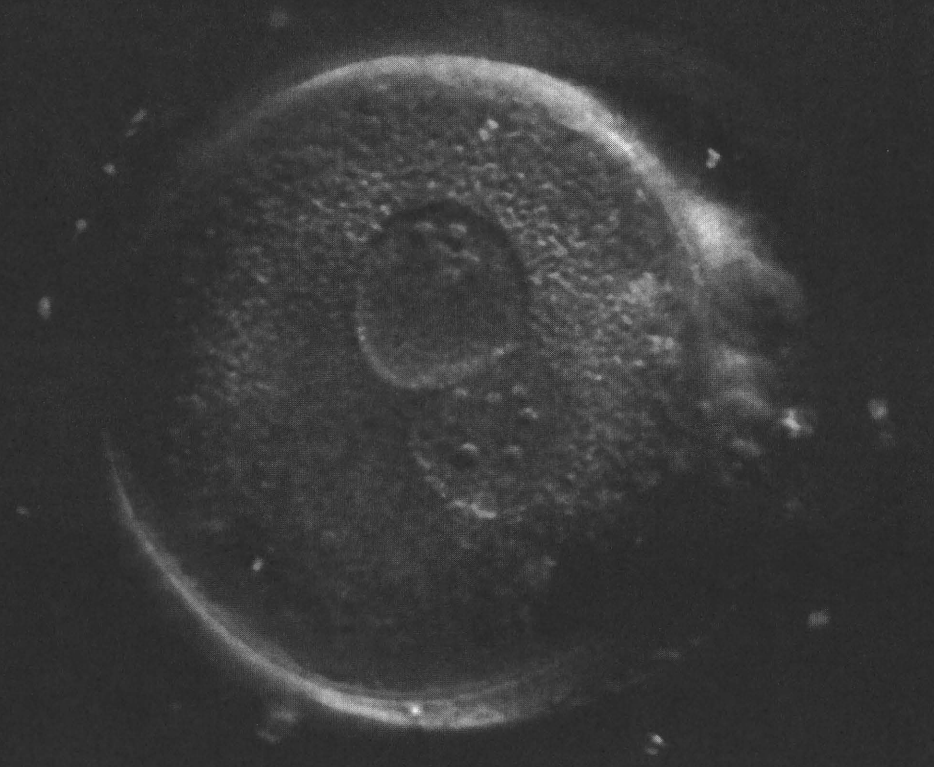

東京化学同人

Hepatology Research

Hepatology Research 2011; **41**: 463–474 doi: 10.1111/j.1872-034X.2011.00784.x

Original Article

Splenectomy reduces fibrosis and preneoplastic lesions with increased triglycerides and essential fatty acids in rat liver cirrhosis induced by a choline-deficient L-amino acid-defined diet

Toshiyuki Oishi,[1] Shuji Terai,[1] Takuya Iwamoto,[1] Taro Takami,[2] Naoki Yamamoto[1] and Isao Sakaida[1]

[1]*Department of Gastroenterology and Hepatology, Yamaguchi University Graduate School of Medicine, and* [2]*Department of Laboratory, Yamaguchi University Hospital, Ube, Yamaguchi, Japan*

Aim: This study investigated whether splenectomy is of significance in non-alcoholic steatohepatitis (NASH).

Methods: Five-week-old Wistar rats were fed a choline-deficient diet for 8 weeks to create a NASH model. A sham-operation or splenectomy was then performed, and rats were killed 4 weeks later.

Results: Liver fibrosis and liver preneoplastic lesions were significantly reduced in the splenectomy group compared to the sham-operation group, and α-smooth muscle actin (SMA) expression was significantly inhibited (liver fibrosis area: sham 8.63 ± 4.09%, splenectomy 5.45 ± 3.69%, $P < 0.01$; preneoplastic lesion size: sham 6.56 ± 3.68 $\times 10^6$ μm²/cm², splenectomy 4.63 ± 3.27 $\times 10^6$ μm²/cm², $P < 0.05$; the number of preneoplastic lesions: sham 8.33 ± 3.96/cm², splenectomy 5.17 ± 1.80/cm², $P < 0.01$; α-smooth muscle actin-positive area: sham 4.41 ± 2.48%, splenectomy 2.75 ± 1.66%, $P < 0.01$) On the other hand, liver triglycerides and essential fatty acids were significantly increased in the splenectomy group (liver triglycerides: sham 182 ± 35.0 mg/g, splenectomy 230 ± 35.0 mg/g, $P < 0.05$; liver linoleic acid: sham 17.2 ± 4.9 mg/g, splenectomy 23.3 ± 6.9 mg/g, $P < 0.05$; liver α-linolenic acid: sham 118 ± 36.6 μg/g, splenectomy 162 ± 51.4 μg/g, $P < 0.05$). In addition, expressions of hepatic fatty acid metabolism-related genes (e.g. acyl-CoA oxidase, liver carnitine palmitoyl-CoA transferase I, cytochrome P450 4A, long-chain acyl-CoA dehydrogenase and medium-chain acyl-CoA dehydrogenase) were significantly inhibited in the splenectomy group.

Conclusion: These findings suggest that spleen plays an important regulatory role in the fibrosis, preneoplastic lesion and lipid metabolism of liver in a rat choline-deficient L-amino acid model.

Key words: fatty acid metabolism, fibrosis, non-alcoholic steatohepatitis, preneoplastic lesion, splenectomy

INTRODUCTION

NON-ALCOHOLIC STEATOHEPATITIS (NASH) is a disease concept first put forward by Ludwig *et al.* in 1980.[1] Despite the absence of a history of alcohol intake sufficient to cause hepatic dysfunction, the pathogenesis of NASH resembles alcoholic liver disease, with progression from simple fatty liver to steatohepatitis and cirrhosis, and ultimately hepatocarcinogenesis.[1] The prevalence of NASH throughout the world is currently increasing. In regard to the etiology of NASH, the two-hit theory proposed by Day *et al.* is currently the most supported theory, stating that fatty liver develops (first hit), followed by the transition to steatohepatitis (second hit).[2] However, the specific mechanisms underlying NASH remain unclear. The first hit of fatty liver is currently thought to develop against a background of so-called metabolic syndrome, with hypertension, dyslipidemia and glucose intolerance, followed by progression to NASH due to some as-yet unknown etiological factor.[2] In addition, NASH can progress to cirrhosis, and ultimately to hepatocellular carcinoma (HCC).

Correspondence: Associate Professor Shuji Terai, Department of Gastroenterology and Hepatology, Yamaguchi University Graduate School of Medicine, 1-1-1 Minami-Kogushi, Ube, Yamaguchi 755-8505, Japan. Email: terais@yamaguchi-u.ac.jp
Received 1 December 2010; revision 9 January 2011; accepted 18 January 2011.

On the other hand, cirrhotic patients occasionally present with hypersplenism, which can result in peripheral cytopenia. Severe peripheral cytopenia may act as a contraindication for aggressive but effective novel therapies, such as interferon therapy or anticancer therapy against HCC with newly developed anticancer drugs, modernized hepatic resection or transplantation.[3] In such cases of hypersplenism, surgical splenectomy is often performed, and postoperative improvements in liver function have been reported.[4,5] Moreover, improved liver fibrosis following splenectomy has been reported in basic research. With regard to underlying mechanisms, splenic-derived transforming growth factor (TGF)-β1, which is thought to stimulate liver fibrosis, may be removed by splenectomy,[6] hepatic tumor necrosis factor (TNF)-α expression may be increased[7] and increased platelet counts may reduce liver fibrosis.[8] Thus, in both basic and clinical studies, splenectomy has been reported to possibly improve liver fibrosis.

Conversely, worsening lipid metabolism due to splenectomy has occasionally been reported. Specifically, rabbits fed a high-cholesterol (high-fat) diet showed decreased high-density lipoprotein cholesterol (HDL-C), increased total cholesterol and triglyceride (TG), and promotion of atherosclerotic changes in the aorta after splenectomy.[9] In addition, rats fed a normal or high-fat diet showed decreased HDL-C and increased TG with splenectomy.[10] In a group of rats fed a normal diet or high-cholesterol diet with subtotal splenectomy, correction of dyslipidemia was reported.[11] In other words, splenectomy may worsen lipid metabolism.

Although the specific etiology of NASH remains unclear, the mechanisms that appear to be involved in the development of this pathology suggest that both fibrosis and lipid metabolism in the liver as factors involved in NASH. However, no studies appear to have described the effects of splenectomy in NASH. This study therefore used a rat choline-deficient L-amino acid (CDAA) diet model (rat steatosis-fibrosis model), as an animal model of NASH,[12,13] to investigate the significance of splenectomy in NASH. We report herein that although splenectomy increased liver TG and essential fatty acids, liver fibrosis and development of preneoplastic lesions were reduced.

METHODS

Animals

MALE WISTAR RATS (5 weeks old, weight 100–120 g; Nippon SLC, Shizuoka, Japan) were quarantined for 1 week, then housed in a room under controlled temperature (25°C), humidity (61–69%) and lighting (12 h light, 12 h dark). Ad libitum access to food and tap water was provided throughout the study period.

Experimental protocol

Rats were divided into two groups: a sham-operation group ($n = 7$) and a splenectomy group ($n = 7$). All rats were fed a CDAA diet for 12 weeks. Eight weeks after beginning the CDAA diet (at 13 weeks old), either a sham-operation (laparotomy and laparorrhaphy without splenectomy) or splenectomy were performed. Four weeks after surgical interventions (at 17 weeks old), all rats were killed. From the start to completion of the study, bodyweight was measured every 4 weeks. At the time of either splenectomy (13 weeks old) or death (17 weeks old), the spleen was weighed.

In addition, we created two normal diet groups: a sham-operation normal diet group ($n = 6$) and a splenectomy normal diet group ($n = 6$). These rats were fed a normal diet from the start to completion of the study. Either a sham-operation or splenectomy were performed at 13 weeks old and all were killed at 17 weeks old.

Measurement of serum markers

Blood samples (5 mL) were obtained from the portal vein at the time of death. White blood cells (WBC), red blood cells (RBC), hemoglobin (Hb) and platelets (Plt) were measured using a KX-21 NV automatic cell counter (Sysmex, Kobe, Japan). Total protein (TP), total bilirubin (T-bil), albumin (Alb), alanine aminotransferase (ALT), aspartate aminotransferase (AST), total cholesterol (T-Cho), TG and HDL-C were measured using an automated analyzer for clinical chemistry (SPOTCHEM EZ SP-4430; Arkray, Kyoto, Japan). TGF-β1 was measured using Immunoassay (enzyme-linked immunosorbent assay; R&D Systems, Minneapolis, MN, USA).

Measurement of triacylglycerol content and fatty acid fractionation in liver tissue

During the 12-week experiment, triacylglycerol content and fatty acid fractionation in liver tissue were measured in all groups. Triacylglycerol in liver tissue was extracted using the method described by Folch *et al.*[14] Fatty acid fractionation in liver tissue was measured using gas chromatography with a flame ionization detector (FID) (GC-17A; Shimadzu, Kyoto, Japan).

Histopathological and immunohistochemical examination

In all experiments, sections (3-μm thick) of the right lobe of all rat livers were fixed in 4% paraformaldehyde phosphate buffer solution, then embedded in paraffin and processed for Sirius-red and immunohistochemical staining. For immunohistochemical analysis, the Vectastain ABC kit (Vector Laboratories, Burlingame, CA, USA) was used to identify anti-α-smooth muscle actin (α-SMA) (dilution 1:300; Abcam, Cambridge, MA, USA), anti-TGF-β1- (dilution 1:100; Santa Cruz Biotechnology, Santa Cruz, CA, USA) and placental-form glutathione *S*-transferase (GST-P)-positive lesions (dilution 1:1000; MBL, Nagoya, Japan) (as preneoplastic lesions) using the avidin–biotin–peroxidase complex method.[15] To estimate Sirius-red-, α-SMA- and TGF-β1-positive areas, MetaMorph software was used for computerized image analysis at ×40 magnification. One section from each liver were prepared for Sirius-red staining, α-SMA and TGF-β1 immunostaining and 10 randomly selected different areas were analyzed per specimen. Positive areas were expressed as the percentage of the total area of the specimen. Three sections from each liver were prepared for GST-P immunostaining. Using a HS all-in-one fluorescence microscope (BZ-9000; Keyence, Osaka, Japan), the section area and preneoplastic lesion area (GST-P-positive area) of each sample were determined. Based on these values, preneoplastic lesion frequency among individuals, and GST-P-positive area per 1-cm^2 section and the number of GST-P-positive lesions per 1-cm^2 section were determined. Data were then compared between groups.

Real-time reverse transcription polymerase chain reaction (RT–PCR) analysis

Total RNA was extracted from each liver using with TRIzol reagent (Invitrogen, Carlsbad, CA, USA) according to the instructions from the manufacturer. Synthesis of cDNA was performed using purified RNA plus random hexamers and the Transcriptor First Strand cDNA synthesis kit (Roche, Indianapolis, IN, USA). All cDNA was stored at −20°C for PCR. Real-time PCR was performed in 20 μL of reaction solution containing 2× Fast SYBR Green Master Mix (Applied Biosystems, California, CA, USA), corresponding primer, sample DNA and d-water. The cycle for PCR was as follows: 1 cycle of 95°C for 20 s; 40 cycles of 3 s at 95°C and 30 s at 60°C; and 1 cycle of 95°C for 15 s, 60°C for 1 min and 95°C for 15 s. Reactions were performed in a Step One Plus real-time PCR system (Applied Biosystems) and amounts of all mRNA were quantified using StepOne ver. 2.1 software (Applied Biosystems). Glyceraldehyde-3-phosphate dehydrogenase (GAPDH) was used as an internal control. For GAPDH and α-SMA, primer sequences were as described by Tajima *et al.*[16] For acyl-coenzyme A oxidase (ACO), liver carnitine palmitoyl-coenzyme A transferase I (L-CPTI), cytochrome P450 4A (CYP4A), long-chain acyl-coenzyme A dehydrogenase (LCAD), medium-chain acyl-coenzyme A dehydrogenase (MCAD), peroxisome proliferator-activated receptor (PPAR)-α, fatty acid synthase (FAS) and sterol regulatory element-binding protein (SREBP)-1c, primer sequences were the same as used by Ringseis *et al.*[17]

Protein extraction and western blotting

Liver samples were obtained from the sham-operation group and splenectomy group. Liver samples (~40 mg) were homogenized in 1 mL of cell lysis buffer (Cell Signaling Technology, Beverly, MA, USA) and a Complete Mini (Roche Diagnostic, Pleasanton, CA, USA) and then were centrifuged. The supernatant represented the whole protein. Next, 40 μg of protein sample was mixed with the same volume of loading buffer (5% 2-mercaptoethanol and 95% Laemmli Sample Buffer [Bio-Rad Laboratories, Hercules, CA, USA]), heated for 3 min at 100°C and separated on 10% sodium dodecylsulfate polyacrylamide gel electrophoresis (SDS-PAGE). Separated bands were transferred to an Immobilon-P transfer membrane (Millipore, Billerica, MA, USA), followed by blocking of the membranes for 1 h with blocking buffer (0.1% Tween-20 [Wako Pure Chemical Industries, Osaka, Japan]), 0.2% I-Block reagent (Tropix, Bedford, MA, USA), and 1 mM Tris-HCl buffer (pH 7.5; Invitrogen). Membranes were then washed with washing buffer (0.1% Tween-20, 1 mM Tris-HCl buffer [pH 7.5]), and incubated for 1 h at room temperature with primary antibodies against α-SMA (Abcam) and β-actin (Abcam) in blocking buffer. After washing, the membrane was incubated for 1 h at room temperature with the appropriate secondary antibodies. Reactive bands were identified using enhanced chemiluminescence (ECL) (Amersham Biosciences, Piscataway, NJ, USA) and autoradiography, in accordance with the instructions from the manufacturers.

Statistical analysis

Statistical significance was determined using Student's *t*-test. Results are presented as the mean ± standard deviation, and differences of $P < 0.05$ were considered significant.

Ethical considerations

This experiment was reviewed by the Committee for Ethics in Animal Experiments of Yamaguchi University Graduate School of Medicine and carried out under the Guidelines for Animal Experiments of Yamaguchi University Graduate School of Medicine and Law no. 105 and Notification no. 6 of the Japanese Government.

RESULTS

Changes in bodyweight

FROM THE START to completion of the study, changes in bodyweight did not differ significantly between groups (Fig. 1a).

Changes in spleen/bodyweight ratios

Spleen/bodyweight ratio at the time of splenectomy (13 weeks old) and spleen/bodyweight ratio at the time of death (17 weeks old) were compared with the spleen/bodyweight ratio in 13-week-old rats fed a normal diet (normal diet group; $n = 8$). Compared to rats on a normal diet, spleen/bodyweight ratios were increased in sham-operation and splenectomized rats at the time of splenectomy and time of death, respectively (normal diet group [13 weeks old], $2.6 \pm 0.4 \times 10^{-3}$; splenectomy [13 weeks old], $5.7 \pm 3.1 \times 10^{-3}$, $P < 0.05$; sham [17 weeks old], $6.4 \pm 1.5 \times 10^{-3}$, $P < 0.01$) (Fig. 1b). Spleen/bodyweight ratios did not differ significantly between the time of splenectomy and the time of death (Fig. 1b).

Blood tests

On blood tests, the splenectomy group showed increased WBC (sham, 6020 ± 1800/μL; splenectomy, $13\,100 \pm 3900$/μL, $P < 0.01$) and increased Plt (sham, $30.3 \pm 8.07 \times 10^4$[/μL]; splenectomy group, $39.6 \pm 12.0 \times 10^4$[/μL], $P < 0.05$). No other blood test results showed any significant difference between groups (Table 1 and Fig. 1c).

Histological and immunohistochemical analysis of α-SMA in liver fibrosis

At 4 weeks after sham operation or splenectomy, histological examination of the liver indicated the presence of liver fibrosis in all rats. Liver fibrosis was measured by estimating extracellular matrix deposition using Sirius-red staining. Results showed that splenectomy extensively decreased the Sirius-red-stained area compared with that in sham-operation rats (Fig. 1d,e). Imaging analysis revealed that splenectomy decreased the percentage Sirius-red-positive area compared with sham-operated rats (sham, $8.63 \pm 4.09\%$; splenectomy, $5.45 \pm 3.69\%$, $P < 0.01$) (Fig. 1f).

Activated hepatic stellate cells, which express α-SMA protein, showed marked proliferation in the livers of sham-operated rats (Fig. 2a). On the other hand, splenectomy groups showed extensively decreased α-SMA-positive areas (Fig. 2b). Quantitative analysis showed that splenectomy significantly reduced the percentage area of α-SMA-positive cells compared with that in the sham-operated group (sham, $4.41 \pm 2.48\%$; splenectomy, $2.75 \pm 1.66\%$, $P < 0.01$) (Fig. 2c).

Western blotting analysis of α-SMA protein in liver

To confirm the inhibitory effect of splenectomy on the activation of hepatic stellate cells, we measured expression of α-SMA protein in the liver by western blot analysis. The splenectomy group showed reduced liver expression of α-SMA protein, compared with the sham-operated group (Fig. 2d).

Real-time RT–PCR analysis of α-SMA mRNA in liver

To confirm the inhibitory effects of splenectomy on activation of hepatic stellate cells, we measured liver expression of α-SMA mRNA by real-time RT–PCR. Livers from the splenectomy group showed reduced expression of α-SMA mRNA, compared with the sham-operated group (sham, 2.12 ± 0.93 [ratio]; splenectomy, 1.18 ± 0.42 [ratio], $P < 0.05$) (Fig. 2e).

Immunohistochemical analysis of TGF-β1 expression in liver fibrosis

Transforming growth factor-β1 expression was also analyzed by immunostaining (Fig. 3a). Splenectomy dramatically reduced TGF-β1 expression (Fig. 3b), and decreased TGF-β1-positive areas in the liver (sham, $6.68 \pm 2.52\%$; splenectomy, $4.21 \pm 2.54\%$, $P < 0.01$) (Fig. 3c), despite no significant difference in plasma TGF-β1 levels between the splenectomy group and the sham-operated group (Fig. 1c).

Effect of splenectomy on GST-P-positive lesions

Preneoplastic lesion (GST-P-positive lesion) frequency among individuals in both groups was 100% (Fig. 3d). However, GST-P-positive area per 1-cm^2 section and the number of GST-P-positive lesions per 1-cm^2 section were significantly decreased in the splenectomy group compared to the sham-operated group (size: sham,

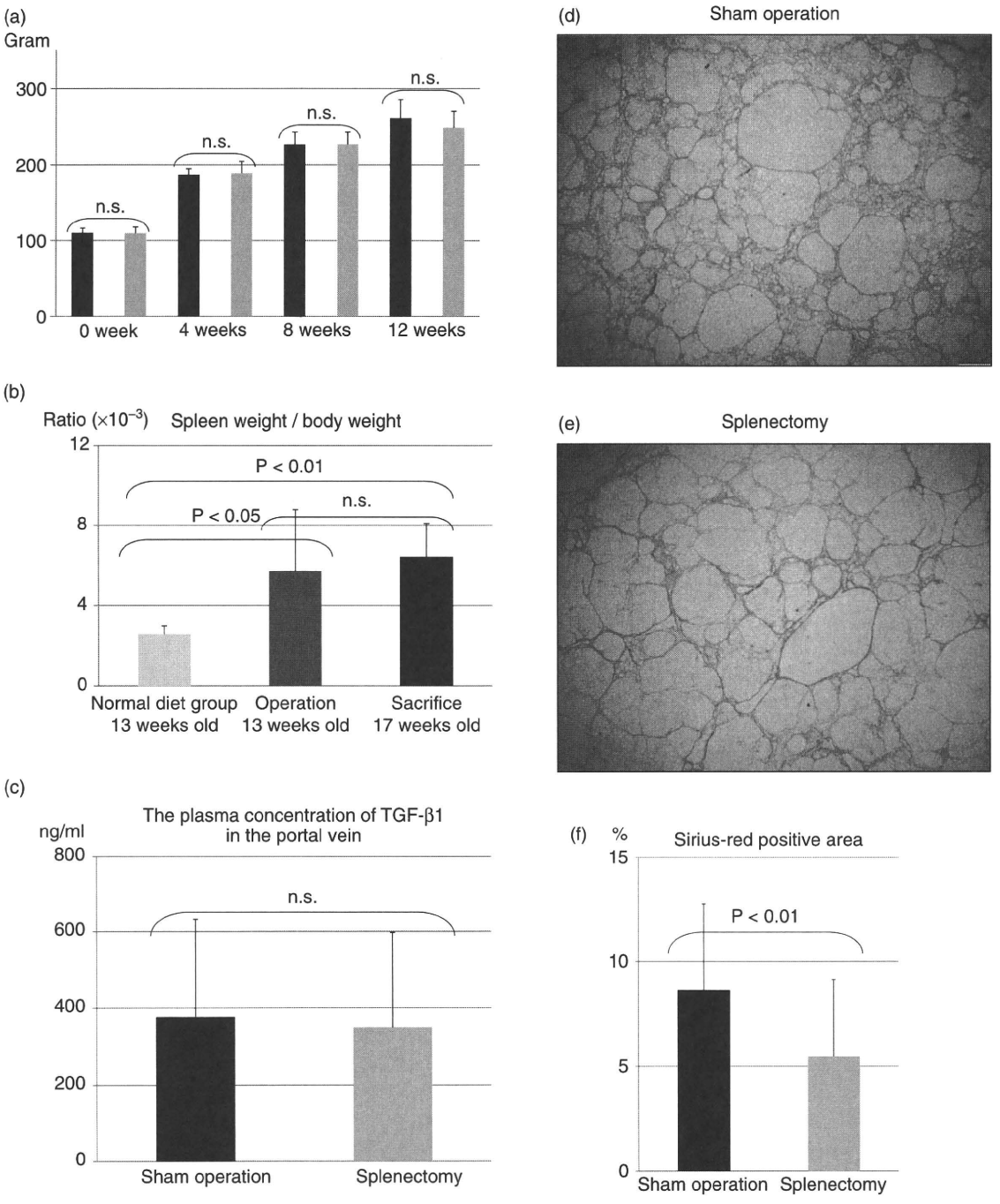

Figure 1 Change in bodyweight from the start to completion of the study (a). Spleen weight/bodyweight ratio (b). The plasma concentration of transforming growth factor (TGF)-β1 in the portal vein (c). Paraffin-embedded liver sections from sham operation, splenectomy rats were performed Sirius-red staining (d,e) (original magnification ×40). Image analysis of Sirius-red-positive areas (f). Data are means ± standard deviation. n.s., no significant difference.

Table 1 Effect of splenectomy on serum markers

	Sham operation	Splenectomy	*P*-value
TP (g/dL)	3.4 ± 0.6	3.9 ± 0.6	n.s.
Alb (g/dL)	1.7 ± 0.36	1.7 ± 0.40	n.s.
T-bil (mg/dL)	0.3 ± 0.1	0.3 ± 0.1	n.s.
ALT (IU/L)	146 ± 62.0	152 ± 65.3	n.s.
AST (IU/L)	294 ± 53.2	330 ± 76.9	n.s.
WBC (/μL)	6 020 ± 1 800	13 100 ± 3 900	<0.01
RBC (/μL)	$617 \pm 34.3 \times 10^4$	$591 \pm 84.0 \times 10^4$	n.s.
Hb (g/dL)	10 ± 0.44	10 ± 10	n.s.
Plt (/μL)	$30.3 \pm 8.07 \times 10^4$	$39.6 \pm 12.0 \times 10^4$	<0.05
T-Cho (mg/dL)	50 ± 0	50 ± 0	n.s.
TG (mg/dL)	41 ± 21	29 ± 9.0	n.s.
HDL-C (mg/dL)	15 ± 3.5	13 ± 5.3	n.s.

Serum markers were measured as described in the text.
Data are means ± standard deviation.
Alb, albumin; ALT, alanine aminotransferase; AST, aspartate aminotransferase; Hb, hemoglobin; HDL-C, high-density lipoprotein cholesterol; n.s., no significant difference; Plt, platelets; RBC, red blood cells; T-bil, total bilirubin; T-Cho, total-cholesterol; TG, triglyceride; TP, total protein; WBC, white blood cells.

$6.56 \pm 3.68 \times 10^6$ μm²/cm², splenectomy, $4.63 \pm 3.27 \times 10^6$ μm²/cm², $P < 0.05$; number: sham, 8.33 ± 3.96/cm², splenectomy, 5.17 ± 1.80/cm², $P < 0.01$) (Fig. 3e,f).

Analysis of triacylglycerol and fatty acid fractionation in the liver

Splenectomy increased liver levels of triacylglycerol (sham, 182 ± 35.0 mg/g; splenectomy, 230 ± 35.0 mg/g, $P < 0.05$) and essential fatty acids (linoleic acid: sham, 17.2 ± 4.9 mg/g, splenectomy, 23.3 ± 6.9 mg/g, $P < 0.05$; α-linolenic acid: sham, 118 ± 36.6 μg/g, splenectomy, 162 ± 51.4 μg/g, $P < 0.05$) compared to sham operation (Fig. 4a–c).

Expression of fatty acid metabolism genes in the liver

Splenectomy reduced the expression of L-CPTI, ACO, CYP4A, LCAD ($P < 0.05$) and MCAD mRNA ($P < 0.01$) (Fig. 4d–h), but did not influence expression of PPAR-α, FAS or SREBP-1c (Fig. 4i–k). There was no significant difference in the expression of L-CPTI, ACO, CYP4A, LCAD and MCAD mRNA between sham-operation and splenectomy normal diet group (Fig. 5a–e).

DISCUSSION

TRANSFORMING GROWTH FACTOR-β1 is a cytokine that causes activation of hepatic stellate cells and stimulates the production of extracellular matrix,[18] and is a major factor for promoting liver fibrosis. In a previous study using a rat model of liver cirrhosis, TGF-β1, produced by splenic macrophages, was reported to possibly inhibit hepatocyte proliferation in damaged liver. Therefore, in the same model, removal of the enlarged spleen was thought to possibly stimulate regeneration of the damaged liver.[6] One potential mechanism underlying the present results could be increased portal blood flow and changes in intrahepatic blood flow, associated with changes in shunt blood flow[4] and changes in TGF-β1 kinetics due to splenectomy.[6]

With a decrease in TGF-β1 expression by splenectomy in the CDAA diet group, hepatic stellate cell activation was inhibited and liver fibrosis improved. Activated stellate cells, which are detected as α-SMA-positive cells and by the expression of α-SMA messenger RNA, cause severe fibrosis as assessed by the hepatic hydroxyproline content. In our previous study,[19] pig serum pretreatment (injection of pig serum into rats induces stellate cell activation resulting in liver fibrosis without parenchymal cell injury) induces more activated stellate cells in the livers of rats subsequently fed a CDAA diet compared with rats fed the CDAA diet alone. Pre-existing fibrosis induced by the activation of stellate cells with pig serum pretreatment has increased hepatic malondialdehyde (MDA) level in parallel with GST-P-positive lesions. These results indicate that pre-existing fibrosis with the activated stellate cells accelerates the development of preneoplastic lesions in a CDAA diet model, so inhibition of hepatocyte stellate cell activation by splenectomy was probably a contributing factor.

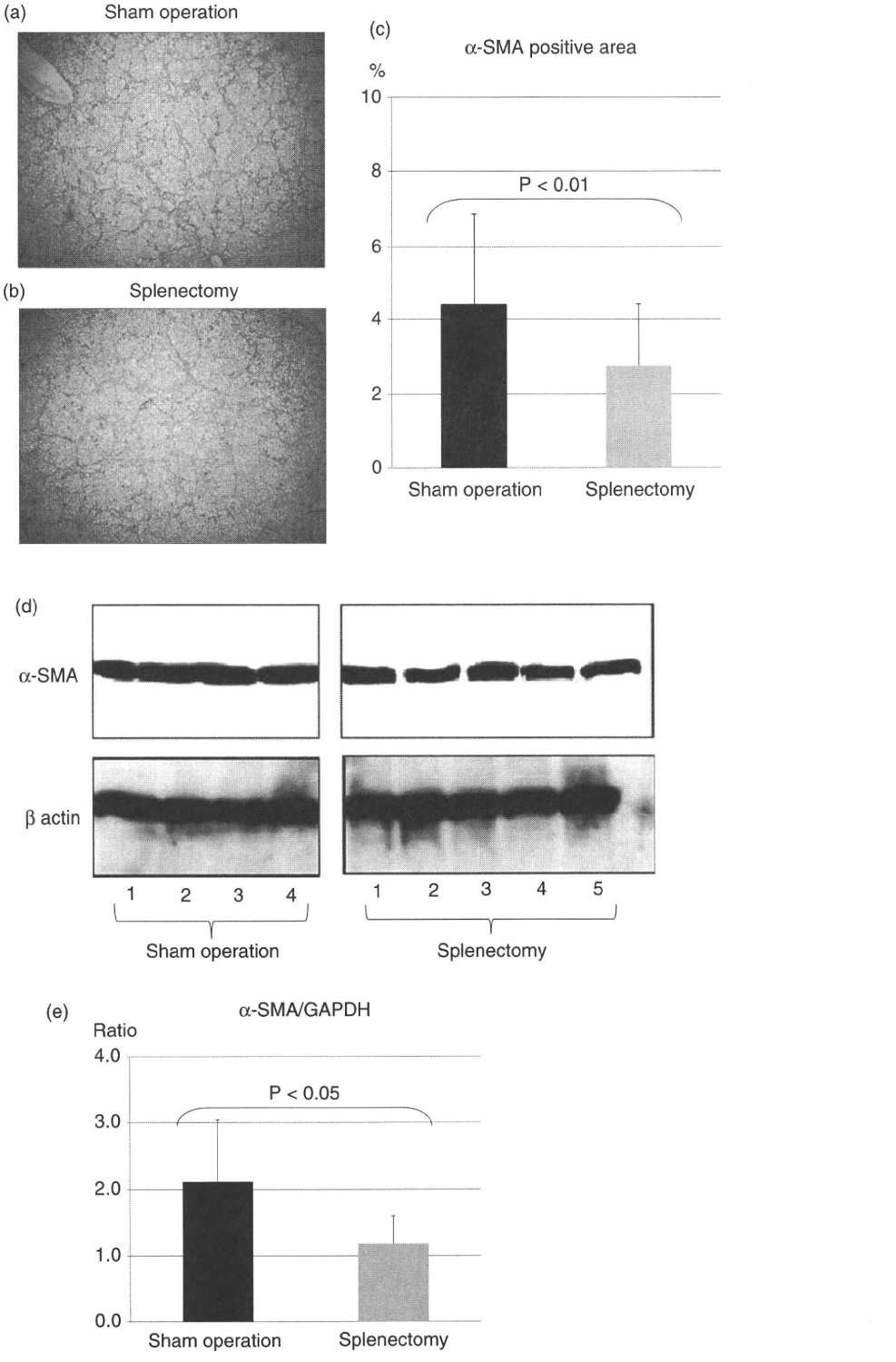

Figure 2 Paraffin-embedded liver sections from sham operation (a) and splenectomy (b) were immunostained for α-smooth muscle actin (α-SMA) (original magnification ×40). Image analysis of α-SMA-positive areas (c). In western blotting, α-SMA expression was inhibited by splenectomy (d). In real-time reverse transcription polymerase chain reaction, mRNA expression of α-SMA was decreased by splenectomy in liver (e). Data are means ± standard deviation. GAPDH, glyceraldehyde 3-phosphate dehydrogenase.

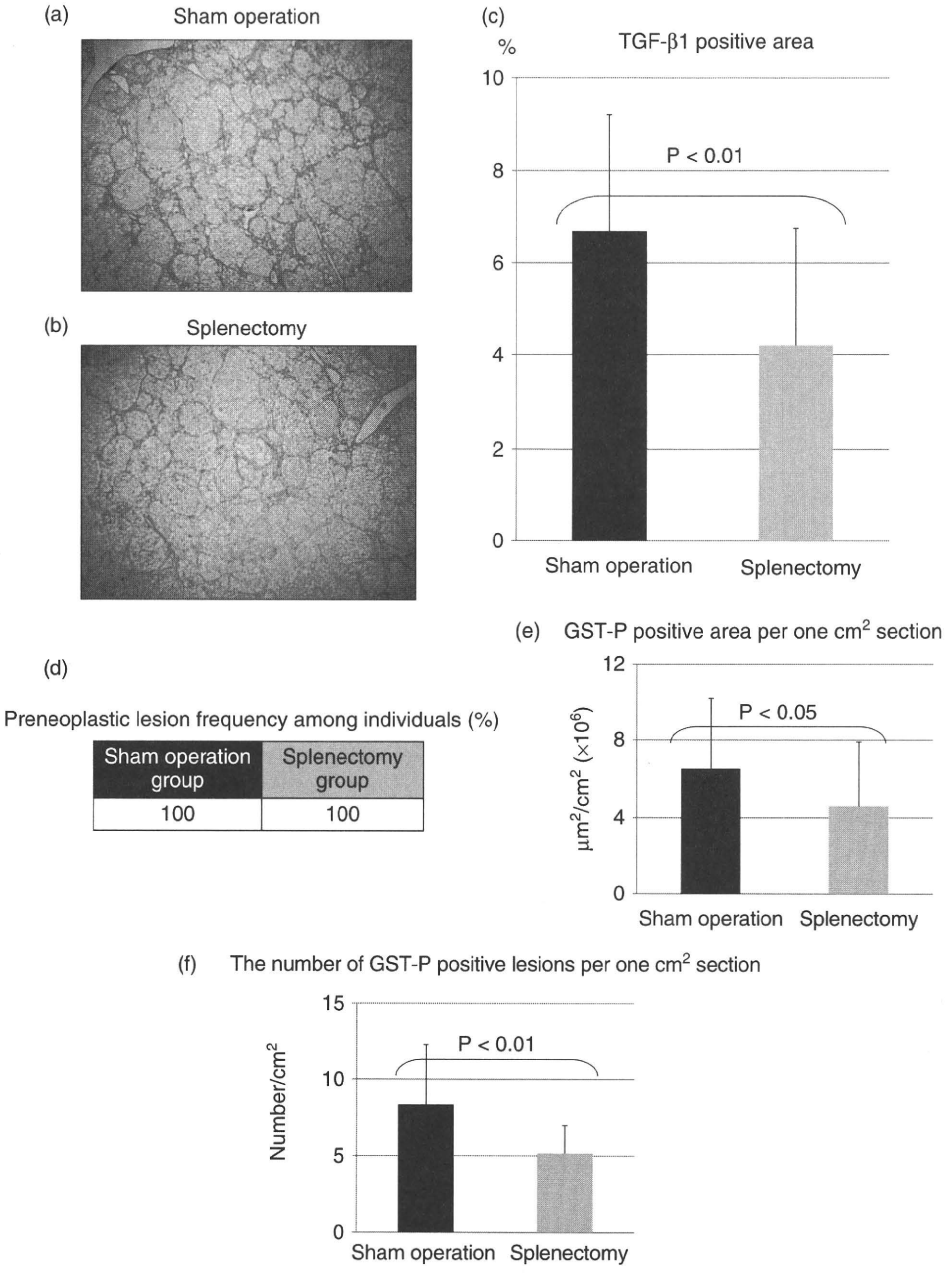

Figure 3 Paraffin-embedded liver sections from sham operation (a) and splenectomy (b) were immunostained for transforming growth factor (TGF)-β1 (original magnification ×40). Image analysis of TGF-β1-positive areas (c). Preneoplastic lesion frequency among individuals (d). Glutathione *S*-transferase (GST-P)-positive area per 1-cm^2 section (e). The number of GST-P-positive lesion per 1-cm^2 section (f). Data are means ± standard deviation.

The mechanism of increased liver fatty acids is thought to be an increase in liver fatty acid synthesis, increased lipid uptake by the liver or decreased liver lipid metabolism. Essential fatty acids are essential for survival of humans and other mammals. These fatty acids cannot be synthesized in the body and must be obtained from the diet.[20,21] Two types of naturally occurring essential fatty acids are used in the body: the ω-6 series derived from *cis*-linoleic acid (LA, 18:2) and the ω-3 series derived from α-linolenic acid (ALA, 18:3).